RSC Advances

PAPER

View Article Online
View Journal | View Issue



Cite this: *RSC Adv.*, 2026, **16**, 17267

# Mechanochemical modification of *Dioscorea* spp. starch: exploring its nano-structural and functional properties for sustainable edible packaging

Valiathan Sreejit and Radhakrishnan Preetha *

Received 13th January 2026
Accepted 24th March 2026

DOI: 10.1039/d6ra00319b

rsc.li/rsc-advances

The current study presents a sustainable mechanochemical method for synthesizing starch nanoparticles from underutilised yams *Dioscorea bulbifera* and *Dioscorea esculenta*. The starch nanoparticles were prepared *via* wet ball-milling (BM) of *Dioscorea bulbifera* starch (DBS) and *Dioscorea esculenta* starch (DES). The influence of mechanochemical alteration upon the structural and techno-functional attributes of DBS and DES was analyzed. SEM revealed that BM resulted in the fragmentation and surface roughening of DBS and DES. The FTIR and Raman spectra confirmed that the BM disintegrated DBS and DES, as evidenced by an increase in the intensity of the FTIR signal at 2932 $cm^{-1}$ and a decrease in the Raman band at 480 $cm^{-1}$. $^{13}C$ NMR and XRD results showed that BM increased the amorphous nature of DBS and DES. BM significantly improved ($p < 0.05$) apparent amylose content, digestibility, oil absorption capacity, water absorption capacity, and significantly reduced ($p < 0.05$) gelatinization enthalpy of DBS and DES. Rheology evaluation showed that BM enhanced the viscoelasticity of DBS and DES. Collectively, these results demonstrate that BM altered the structural and techno-functional attributes of DBS and DES, thereby enabling them to be employed as fillers in sustainable edible packaging.

## 1. Introduction

Starch is an abundant, eco-friendly, and natural carbohydrate polymer alternative to existing petroleum-based plastics.[1] It is intrinsically biodegradable due to the presence of glycosidic bonds, which can be broken down with natural enzymes, such as amylase, or other hydrolases.[2–4] As the food industry focuses on reducing its carbon footprint to comply with environmental regulations, the use of starch for sustainable packaging is on the rise.[5] Native starch granules are water-insoluble, largely inert, have limited resistance to shear forces,[6,7] and are also hydrophilic.[8] Thus, starch needs to be modified to be employed in food packaging.

One strategy to surpass these limitations inherent to native starch is to convert the starch into starch nanoparticles (SNPs). SNPs are particles of starch that have a size smaller than 1000 nm.[7] They have already been widely used in food packaging, bioactive compound encapsulation, nanocomposite films, and pickering emulsion stabilizers.[7] The nanoscale fabrication of starch decreases its agglomeration and improves the mechanical attributes of the packaging.[9] They are promising fillers in food packaging, as they enhance the barrier, physical, and mechanical properties, as well as the biodegradability of food packaging.[1] SNPs prepared through jet cavitation followed by enzymolysis were reported to augment the impermeability and flexibility of food packaging.[10] SNPs exhibit increased water absorption capacity due to their increased surface area.[7,9] SNPs exhibit high encapsulation effects and bioavailability.[11] Nanoparticles prepared from renewable biopolymers such as cellulose and starch facilitate the fabrication of eco-friendly food packaging.[1]

The starch is mainly modified through physical, chemical, or enzymatic methods.[12,13] There is a marked rise in consumer preference towards environmentally friendly and clean-label products.[14] Physical modifications of starch are generally more cost-effective and safer than alternative treatments.[15,16] BM exerts mechanical forces that change the molecular size and crystalline nature of starch. These modifications enhance the digestibility and solubility of starch.[17] Physical modification also displays similar changes in functional groups of starch, avoiding chemical reagents, which can often be toxic, and does not produce effluents with unwanted reagents or by-products.[18,19] Green nanoparticle synthesis is gaining popularity due to its sustainability and diverse applications in medicine and food technology.[9] Commonly used green techniques for the preparation of SNPs are ball-milling (BM), high-pressure homogenization, mini emulsion cross-linking, cold plasma treatment, electrospraying, and electrospinning.[20–23]

BM of starch is reported to be a mechanochemical modification process, since the mechanical forces of BM bring about various structural and physicochemical transformations in starch. BM alters the properties of starch through

*Department of Food Technology, School of Bioengineering, Faculty of Engineering and Technology, SRM Institute of Science and Technology, SRM Nagar, Kattankulathur, Chengalpattu District, Chennai, 603203, India. E-mail: preethar@srmist.edu.in*

fragmentation and amorphization of starch.[24,25] Juarez *et al.* observed that BM mechanolysed potato starch, cleaving the glycosidic bond of potato starch.[26] The effectiveness of mechanolysis of polymer chains during BM, depends on the occurrence of weak chemical bonds, configuration of the polymer, and strength of the polymer chains.[27] BM alters the morphology and ordered structure of the starch molecule, thereby tailoring the functional attributes of starch.[28] BM reduces the final sample size by the collision of the blending balls.[29] Increasing the milling energy decreases the particle size, crystallinity degree, and gelatinization enthalpy.[30] BM reduces the gelatinization enthalpy of starch, thereby enabling the modified starch to form a thin, flexible film.[31] Physical modification techniques were employed in earlier studies to improve the functional characteristics of starch from water chestnut, lotus stem, horse chestnut,[28] pearl millet, proso millet.[32] foxtail millet, sorghum,[33] and corn[31] for enabling their application as functional food additives. Wet BM uses surface-active media to inhibit the formation of aggregates.[34] Wet BM is efficient in modifying starch granules.[35] Wet BM mitigates dust and heat generation and makes finer particles.[36] BM provides a simple, cost-effective, and sustainable physical approach for starch modification that facilitates convenient scaling up from the laboratory to commercial applications.[14,23] The BM technique has a distinctive characteristic: scaling up samples for large-scale manufacturing is not challenging. The mechanochemical modification of starch affects both the fragmentation and accumulation properties of starch. BM enhances the chemical reactivity of the sample, which ultimately determines the product and its characteristics. A critical physical factor in both lab-scale and commercial BM is the kinetic energy of the balls with a known weight, moving at the agitation velocity. The kinetic energy affects the efficacy and the overall time required for particle comminution.[34]

Diverse milling equipment is used for different-scale mechanochemical modification of biomass. The mixer mills are used for mechanochemical modification at the gram scale and are appropriate for lab-scale studies. For larger quantities, planetary BM is employed. On the other hand, stirred media BM are employed for commercial-scale mechanochemical modification of biomass. For instance, the Outotech HIG mill handle quantities greater than 1 tonne.[37]

Potatoes, rice, wheat, and corn are the primary sources of starch. However, the rising commercial need for starch has prompted the exploration of underexploited starch sources, such as rhizomes, tubers, and seeds.[38] Leveraging underused starch sources offers an opportunity to expand the range of plant sources for SNP synthesis,[1] hence minimizing global dependence on commonly used raw materials and promoting food security.[39]

The air potatoes (*Dioscorea bulbifera*) are a type of underused yam.[40] *D. bulbifera* exhibits distinctive, irregularly shaped starch granules with a triangular and oval morphology.[41–43] It has an average starch content of 62.70%, which includes an average of 19.53% amylose and 43.17% amylopectin.[44] It shows a B-type crystalline pattern, with a hexagonal lattice framework.[41,45,46]

*Dioscorea esculenta* is an underused yam,[47] and it has an average starch content of 59.8% that comprises an average of 9.73% amylose and 50.07% amylopectin.[44] It also shows a B-type crystalline pattern, with a hexagonal lattice framework.[45,46] Currently, there is no research on the sustainable nanoscale fabrication of DBS and DES.

Yam (*Dioscorea* spp.) starches have higher gelatinization enthalpy and temperatures than wheat, potato, tapioca, and corn starches, possibly due to variations in size, morphology, and amylose content.[48] In this context, modification of DBS and DES is necessary to reduce their gelatinization enthalpy, and thereby enhance the processability to form homogenous, transparent edible films with improved flexibility. In contrast to commonly used starch sources such as potato, corn, taro, and millet, the utilization of underutilized starch sources *Dioscorea bulbifera* and *Dioscorea esculenta* provides a sustainable source of starch, contributing to a resilient food supply by diversifying starch sources.

In this study, it is hypothesized that the sustainable mechanochemical modification of starch extracted from *Dioscorea bulbifera* and *Dioscorea esculenta via* planetary wet BM may enhance the structural properties, dispersibility, viscoelasticity, amorphicity, digestibility, and processability of DBS and DES, thereby improving their potential as fillers for flexible edible packaging. This is the pioneering study that focuses on the effect of sustainable mechanochemical modification of starch from underutilized yams (DBS and DES) using BM on their microstructural and functional properties. The outcomes of this study will add to the growing research on green and sustainable approaches to modify starches and offer insights into the potential of nanoscale-fabricated yam starches for flexible edible packaging.

## 2. Materials and methods

### 2.1. Materials

Fresh tubers of air potato (*Dioscorea bulbifera*) and lesser yam (*Dioscorea esculenta*), exhibiting uniform size and shape (SI Fig. 1), devoid of any mechanical or pathological injuries, were procured from a local farm in Kottayam, Kerala, India. The tuber samples were peeled, sliced, rinsed in 0.02% w/v sodium metabisulfite solution for 15 minutes, air-dried, and refrigerated. Analytical grade reagents were utilized in the study.

### 2.2. Extraction of starch from *Dioscorea bulbifera* and *Dioscorea esculenta*

Starch extraction from *Dioscorea* spp. was carried out as described in the literature with slight modifications.[47] *Dioscorea bulbifera* was ground for 1.5 minutes. Twenty-five percent w/v of crushed *Dioscorea bulbifera* was dispersed in a 0.02% w/v sodium metabisulfite solution and filtered through cheesecloth. The filtrate was refrigerated at 4 °C for 3 hours to promote sedimentation, then washed twice with distilled water. Subsequently, the suspension was refrigerated for 30 hours to allow the starch to settle completely, oven-dried at 50 °C, ground for 2 minutes to obtain a fine powder, and sieved through a 60 mesh

screen (250 μm pore size) to obtain *Dioscorea bulbifera* uniform-sized finer starch powder (SI Fig. 2). The same procedure was used to extract starch from *Dioscorea esculenta.*

### 2.3. Preparation of starch nanoparticles by wet ball-milling

*Dioscorea* spp. starch nanoparticles were synthesized in a BM equipment (planetary mono classic line Pulverisette 6, Fritsch GmbH, Germany). The parameters of ball-milling of DBS and DES, such as starch: ball weight ratio, ball-milling speed, and duration, were chosen based on the literature.[31] The prior optimization was using the one-factor-at-a-time technique (SI Fig. 3 and 4). DBS was comminuted with 10 mm tungsten carbide balls at 1 : 10 DBS : ball w/w ratio, at 300 rpm for 3 h, whereas DES was ball-milled at 1 : 12 DES : ball w/w ratio, at 300 rpm for 3 hours. Ethanol was used to uniformly disperse starch during ball milling at a 1 : 10 starch-to-ethanol ratio.[49] The procedure was halted for fifteen minutes every thirty minutes. For future analysis, the ball-milled DBS (SI Fig. 2), and ball-milled DES (SI Fig. 2) were preserved at 4 °C.[50]

### 2.4. Structural analysis of raw and nanoscale fabricated DBS and DES

#### 2.4.1. Morphological characterization

*2.4.1.1. Scanning electron microscopy.* The morphological characterization of raw and ball-milled DBS and DES were performed using a scanning electron microscope (SEM, TESCAN, X-FLASHR 6/30 SDD Detector, VEGA-3-QUANTAX 2000, Berlin, Germany) at 10 kV. Samples were laminated with a thin chromium film using plasma sputtering for improved conductivity during examination. A high-resolution camera installed in the SEM captured the images.[51]

*2.4.1.2. Transmission electron microscopy.* The morphological characteristics of the raw and ball-milled DBS and DES were verified by TEM (JEOL, JEM-1200 Plus, Japan) on Cu grid at 300 kV. The sample images were taken using a CCD camera, and the statistical dimensional analysis of the DBS, DES, DBNS, and DENS was done using ImageJ software and Origin software.[52]

**2.4.2. Measurement of particle size and polydispersity index (PDI).** The particle size and PDI of 0.01% w/v each of DBS, DBNS, DES, and DENS dissolved in de-ionized water were evaluated using Zeta sizer (Malvern/Nano ZS-90) at neutral pH and 25 °C.[32]

**2.4.3. X-ray diffraction analysis.** The XRD pattern of raw and ball-milled DBS and DES was obtained using an X-ray diffractometer (XRD, XPERT-PRO, Copper Kα, 30 mA, 40 kV). The XRD investigations were conducted within $2\theta$ (angular region) from 5 to 100°, using a step increment of 0.0110° with a duration of 97 seconds for each step. The Rietveld refinement technique was done using the GSAS-II software to refine crystallographic parameters obtained from XRD patterns.[53] The Rietveld refinement technique was used to determine the crystallinity and apparent crystallite size, in accordance with Pinto *et al.*[54]

**2.4.4. Fourier transform infrared (FTIR) spectroscopy and Raman spectroscopy (RS).** Fourier transform infrared (FTIR) spectroscopy (Agilent Cary 660/670, Santa Clara, United States of America) with 4 $cm^{-1}$ spectral resolution and a spectral frequency of 4000–400 $cm^{-1}$ range was used to identify the organic functional groups of raw and ball-milled DBS and DES.[55]

The structure and composition of raw and ball-milled DBS and DES were further examined using a high-resolution laser RS (LABRAM HR Evolution, Horiba, Kyoto, Japan), at a wavelength of 633 nm, and a scanning range of 500–4000 $cm^{-1}$.[56]

**2.4.5. $^{13}C$ cross-polarization/magic angle spinning nuclear magnetic resonance (CP/MAS NMR) spectroscopy.** The solid-state $^{13}C$ NMR studies of the raw and ball-milled DBS and DES were performed using the spectrometer (AVANCE III HD 400 MHz, Bruker, Karlsruhe, Germany), employing the CP/MAS method, with a cross-polarization contact duration of 1.2 ms, acquisition period of 25.17 ms, and more than 1000 scans per spectrum.[57] Origin software (Origin Pro 2021) was used to deconvolute and evaluate the relative amounts of amorphous portions and single- and double-helix components in the raw and ball-milled starch samples.

### 2.5. Evaluation of techno-functional properties of raw and nanoscale fabricated DBS and DES

**2.5.1. Colour analysis.** The color of the raw and ball-milled DBS and DES was measured utilizing a Hunter Lab colorimeter (Color Quest Di8-XE; Hunter Associates Laboratory, USA). The lightness ($L^*$), red-green ($a^*$), and yellow-blue ($b^*$) were analyzed using the CIE lab-scale.[32] Whiteness index of the samples was evaluated using $L^*$, $a^*$, and $b^*$ readings.[58]

**2.5.2. Thermal analysis.** The thermal characteristics of raw and ball-milled DBS and DES samples were evaluated with the help of a differential scanning calorimeter (PerkinElmer, Simultaneous Thermal Analyzer STA 8000—USA) under $N_2$. 10 mg of the raw and ball-milled starches were placed in platinum pans, along with deionized water (8 μL), and heated from an initial temperature of 10 °C to a final temperature of 240 °C, at a constant temperature gradient of 10 °C $min^{-1}$.[32]

**2.5.3. Apparent amylose content (AAC).** The AAC of the raw and ball-milled DBS and DES was determined using iodine and spectrophotometric techniques.[59] 0.1 g of the raw and ball-milled starch samples was dispersed in 1 mL of ethanol, and 10 mL of 1 N NaOH was added, heated for 10 minutes, and diluted. 3 mL of this test sample mixture was mixed with 20 mL of deionised water, a few drops of phenolphthalein solution, and 1 mL of $I_2$ solution. It was then diluted to 50 mL. The spectrophotometric reading of these samples was taken at 590 nm. The amylose in the raw and ball-milled samples was quantified using the standard curve of amylose using the following equation as described in the literature.[59]

$$\%\ \text{Amylose} = \left\{\frac{t}{3}\right\} \times 100\% \quad (1)$$

where "$t$" is the concentration of amylose of test samples obtained from the standard curve of amylose, based on their absorbance readings at 590 nm.

**2.5.4. Rheology evaluation.** Starch gels were prepared by gelatinizing 6% (w/v) each of raw and ball-milled DBS and DES in water for 20 minutes at 90 °C with continuous stirring. The Antonpar rheometer (MCR 502, Anton Paar GmbH, Austria) was utilized to find out the viscosity of the gels at 25 °C on a parallel

plate (PP 25, diameter 25 mm, gap 1 mm) after it had cooled to room temperature. The frequency test of the starch gels was performed at a strain of 1%, at 25 ± 0.1 °C, and an angular frequency of 0.1 to 100 rad $s^{-1}$.[60] The shear stress sweep test of the starch gels was done at 25 ± 0.1 °C, at a steady frequency of 1 Hz, and shear rate from 0.1 to 100 $s^{-1}$ to find out the viscoelastic range of the starch gels.[28]

**2.5.5. Water absorption capacity (WAC) and oil absorption capacity (OAC).** Raw and ball-milled starch from DBS and DES (5% w/v) were blended with distilled water/sunflower oil, and uniformly mixed. They were centrifuged at 5000 rpm for 15 minutes (5810R, Eppendorf, Hamburg, Germany). The supernatant was gradually emptied. The WAC and OAC were evaluated by measuring the weight gain of the sample after centrifugation.[28]

**2.5.6. Evaluation of digestive properties.** *In vitro* digestion studies of raw and ball-milled starch were done for quantifying Rapidly Digestible Starch (RDS), Slowly Digestible Starch (SDS), and Resistant Starch (RS) in accordance with Englyst *et al.*[61] 400 mg of DBS, DES, DBNS, and DENS were taken in separate centrifuge tubes, pretreated with pepsin at 37 °C, and neutralized. Then the pH of the samples was adjusted to 5.2 and digested with α-amylase (290 units per mL)/glucoamylase (50 units per mL) at 120 rpm at 37 °C. During enzyme digestion, at regular intervals (0, 20, and 120 minutes), 1 mL of enzyme-digested solution was collected, and inactivated with ethanol. This solution was then centrifuged for 10 minutes at 4000 rpm. The glucose present in the supernatant from each sample was measured spectroscopically using the DNS (dinitrosalicylic acid) technique. The amount of RDS, SDS, and RS present in the raw and ball-milled samples was evaluated using the equations below.[36]

$$\mathrm{RDS} = [(\mathrm{GLU}_{20} - \mathrm{GLU}_0)/m_s] \times 0.9 \times 100\% \quad (2)$$

$$\mathrm{SDS} = [(\mathrm{GLU}_{120} - \mathrm{GLU}_{20})/m_s] \times 0.9 \times 100\% \quad (3)$$

$$\mathrm{RS} = 100 - (\mathrm{RDS} + \mathrm{SDS})\% \quad (4)$$

$GLU_0$, $GLU_{20}$, and $GLU_{120}$ denote the amount of glucose present in the samples after 0, 20, and 120 minutes of enzymatic digestion, respectively. $m_s$ is the mass of the sample taken for digestion. 0.9 is the coefficient that corresponds to the transformation of glucose into starch. It is obtained by dividing the molecular weight of starch (162 g $mol^{-1}$) monomer by that of glucose (180 g $mol^{-1}$).[36]

## 2.6. Application study of DBNS and DENS in potato starch-based edible films and characterization of its mechanical properties

Edible films were prepared by mixing 5% w/v potato starch and plant-based glycerol (30% w/w of potato starch) in distilled water, then placed on a hot plate magnetic stirrer and stirred at 65 °C and 800 rpm for 30 minutes to ensure complete gelatinization. This edible film-forming solution was then cooled to 40 °C before starch nanoparticles were incorporated. Subsequently, each of DBNS and DENS was added at concentrations of 1, 2, and 3% w/w of potato starch, respectively, to the potato starch-based edible

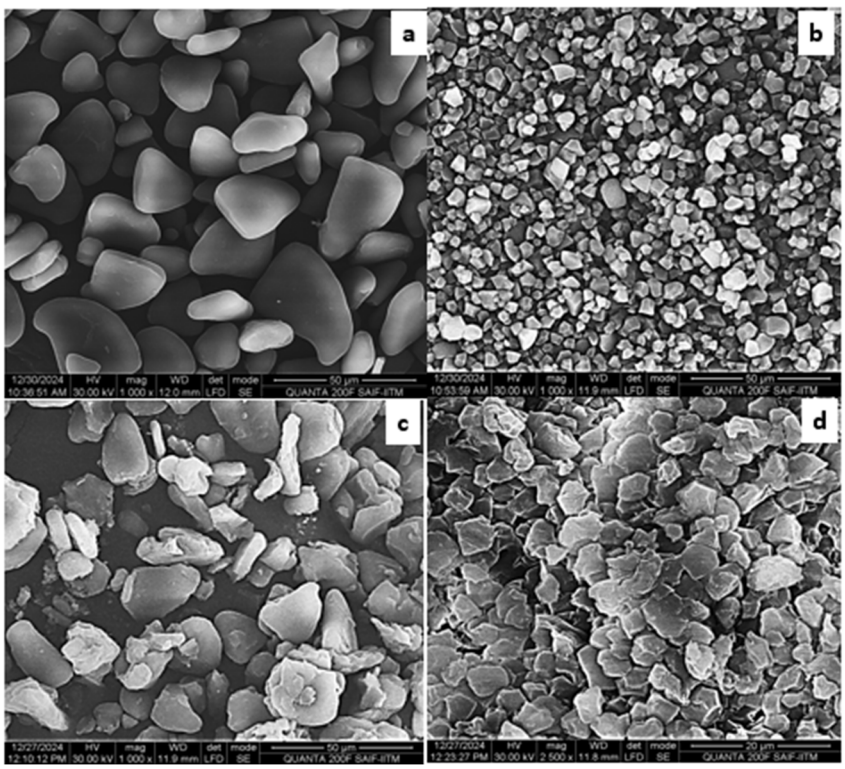


Fig. 1 SEM images depicting the effect of BM on DBS and DES. (a) Raw *Dioscorea bulbifera* starch, (b) raw *Dioscorea esculenta* starch, (c) DBNS, and (d) DENS.

 

film-forming solution, stirred at 800 rpm for 20 minutes to ensure uniform mixing. The edible film-forming solution without starch nanoparticles was used as the control sample. Then, 50 mL of each edible film-forming solution was poured onto casting plates of diameter 15 cm, and dried at 33 ± 1 °C overnight. The dried edible films were then peeled off the casting plate and stored at ambient temperature for characterization studies. The tensile strength and elongation at break of the prepared edible films were tested using ASTM D882.[51]

### 2.7. Statistical analysis

Data analysis was conducted using one-way analysis of variance (ANOVA) in the SPSS statistical package (SPSS Statistics for Windows, version 29) to identify significant differences in the parameters. The values are specified as the means ± standard deviation of triplicate readings. Tukey's Honest Significant Difference test was employed for multiple comparisons at a 0.05 significance level.[62]

## 3. Results and discussion

### 3.1. Structural analysis of raw and nanoscale fabricated DBS and DES

#### 3.1.1. Morphological characterization

*3.1.1.1. Scanning electron microscopy.* The effect of BM on the morphological characteristics of DBS and DES was studied using SEM. Fig. 1 displays the results of SEM of raw and ball-milled DBS and DES. The raw DBS were triangular, and the raw DES were polygonal. BM altered the shape of both raw starches. SEM images showed that the mechanical forces of BM, led to fragmentation and increased surface roughness in DBS and DES. BM altered the microscopic morphology of starch through various mechanical forces, including shear, friction, impingement, and impact.[23] These mechanical forces involved in BM rupture the integrity of DBS and DES and reduce their particle size. The grinding forces of BM break up bigger starch particles and create reactive contacts between the sample particles. Then the kinetic energy of the balls activates the reactive contacts, which will disrupt the intermolecular hydrogen bonds of DBS and DES, resulting in sample deformation.[63] BM enhances the surface area/volume of the starch and thereby alters its physicochemical and functional attributes.[17] It has been reported that BM resulted in the fragmentation and roughening of proso and pearl millet starch,[32] wheat starch,[64] and taro starch.[14] The reduced particle size of SNPs improves their barrier properties, mechanical properties, and biodegradability, making them promising candidates for use in edible packaging.[1]

*3.1.1.2. Transmission electron microscopy.* The size and morphology of raw DBNS and DENS were confirmed using TEM analysis. Fig. 2 depicts the TEM images of DBS, DBNS, DES, and DENS. The average particle size (APS) of DBNS and DENS was evaluated using the ImageJ software. The data obtained from

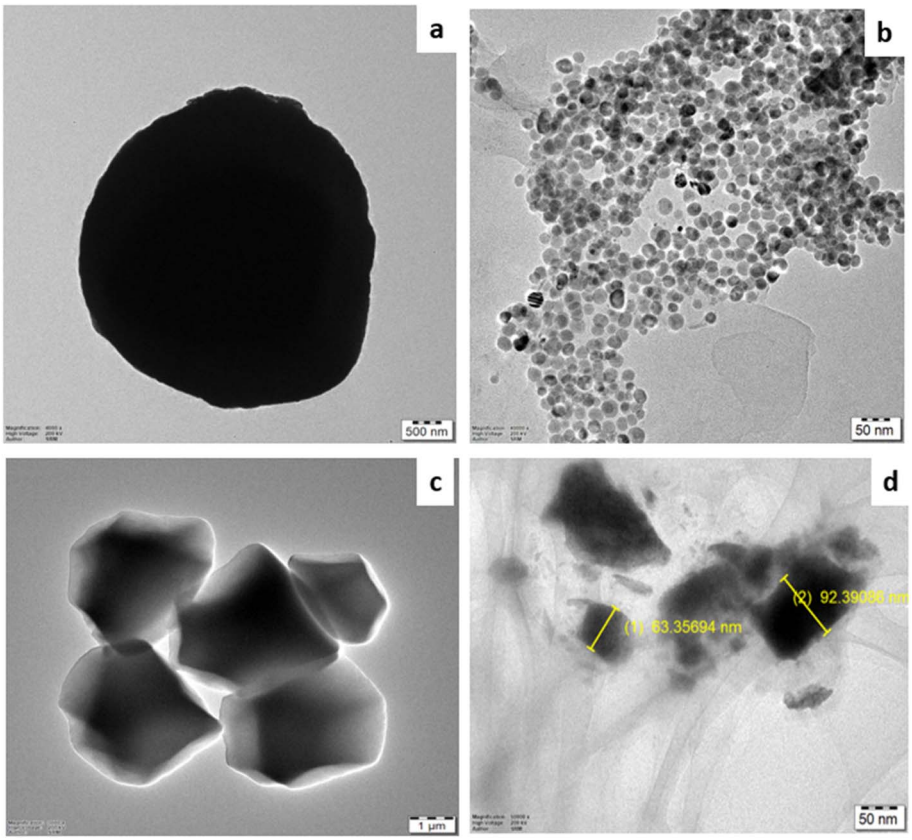


Fig. 2 TEM images depicting the effect of BM on DBS and DES (a) raw *Dioscorea bulbifera* starch, (b) ball-milled *Dioscorea bulbifera* starch, (c) raw *Dioscorea esculenta* starch, and (d) ball-milled *Dioscorea esculenta* starch.

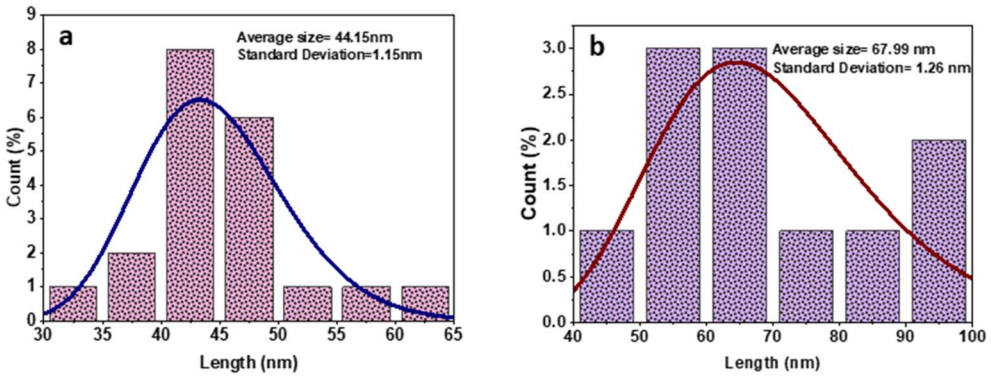


Fig. 3 Particle size distribution for (a) ball-milled *Dioscorea bulbifera* starch, and (b) ball-milled *Dioscorea esculenta* starch fitted with a log normal distribution function.

the ImageJ software was analyzed by plotting on a histogram using the Origin software. SNPs were randomly measured throughout the TEM images of DBNS and DENS using the ImageJ software. The diameter lengths were noted in Microsoft Excel. The histogram with a log-normal distribution curve plotted using Origin software with the data set is shown in Fig. 3. From the data set, the APS of DBNS and DENS were calculated using the statistics tool in Origin, and the values of APS obtained for DBNS and DENS were 44.15 ± 1.15 nm and 67.99 ± 1.26 nm, respectively.

TEM results showed that the mechanical forces of BM led to the rupture and surface roughening of DBS and DES, thereby improving their dispersion. During the BM of DBS and DES, the kinetic energy from the collision between the ball, starch, and the ball milling equipment wall gets converted into mechanical forces such as shear and frictional forces. These mechanical forces selectively disrupt α-1,6 glycosidic bonds of amylopectin subunits within the starch molecules.[65] Previous studies reported that BM led to fragmentation, surface roughening, and enhanced dispersion of waxy corn starch,[66] and potato starch.[67] Consequently, it became apparent that BM fragmented DBS and DES and improved their dispersion.

**3.1.2. Measurement of particle size and polydispersity index (PDI).** A Zeta sizer assessed the random Brownian motion

Table 1 Physicochemical, functional, thermal, and digestive properties of raw and ball-milled DBS and DES[a]

| | DBS | DBNS | DES | DENS |
|---|---|---|---|---|
| **Parameter** | | | | |
| Average particle size (nm) | 1019 ± 32.5$^{b}$ | 243 ± 15.5$^{d}$ | 1413 ± 33.5$^{a}$ | 641 ± 24.5$^{c}$ |
| PDI | 0.746 ± 0.05$^{b}$ | 0.479 ± 0.06$^{d}$ | 0.908 ± 0.05$^{a}$ | 0.614 ± 0.04$^{c}$ |
| **Techno-functional properties** | | | | |
| WAC (g g$^{-1}$) | 1.18 ± 0.08$^{b}$ | 1.46 ± 0.06$^{a}$ | 1.23 ± 0.04$^{b}$ | 1.54 ± 0.11$^{a}$ |
| OAC (g g$^{-1}$) | 1.43 ± 0.06$^{b}$ | 1.78 ± 0.19$^{a}$ | 1.21 ± 0.05$^{c}$ | 1.48 ± 0.14$^{b}$ |
| **Colour** | | | | |
| $L^*$ | 78.84 ± 0.68$^{b}$ | 71.69 ± 0.33$^{c}$ | 92.35 ± 0.87$^{a}$ | 69.53 ± 0.56$^{d}$ |
| $a^*$ | 0.44 ± 0.04$^{b}$ | 0.76 ± 0.07$^{a}$ | −3.61 ± 0.09$^{d}$ | −0.93 ± 0.19$^{c}$ |
| $b^*$ | 17.03 ± 0.18$^{b}$ | 20.08 ± 0.77$^{a}$ | 4.39 ± 0.36$^{d}$ | 9.29 ± 0.74$^{c}$ |
| WI | 72.83 ± 0.55$^{b}$ | 65.28 ± 0.70$^{d}$ | 90.47 ± 0.87$^{a}$ | 68.13 ± 0.67$^{c}$ |
| **Thermal** | | | | |
| Onset temperature (°C) | 48.8 ± 0.45$^{c}$ | 45.7 ± 0.53$^{d}$ | 62.3 ± 0.38$^{a}$ | 54.2 ± 0.65$^{b}$ |
| Peak temperature (°C) | 84.29 ± 0.31$^{b}$ | 78.9 ± 0.22$^{d}$ | 101.9 ± 0.57$^{a}$ | 81.78 ± 0.19$^{c}$ |
| Conclusion temperature (°C) | 146.4 ± 0.57$^{c}$ | 140.5 ± 0.43$^{d}$ | 164.9 ± 0.62$^{a}$ | 149.6 ± 0.35$^{b}$ |
| Enthalpy (J g$^{-1}$) | 206.1 ± 0.62$^{b}$ | 194.5 ± 0.83$^{c}$ | 290.4 ± 0.47$^{a}$ | 174.9 ± 0.35$^{d}$ |
| Apparent amylose content (%) | 17.85 ± 0.36$^{b}$ | 25.64 ± 0.45$^{a}$ | 9.21 ± 0.50$^{d}$ | 15.36 ± 0.28$^{c}$ |
| **Digestive properties** | | | | |
| RDS (%) | 23.76 ± 0.85$^{d}$ | 47.56 ± 0.47$^{c}$ | 50.18 ± 0.92$^{b}$ | 67.86 ± 1.09$^{a}$ |
| SDS (%) | 18.53 ± 0.68$^{a}$ | 6.83 ± 0.48$^{c}$ | 15.87 ± 0.45$^{b}$ | 3.28 ± 0.21$^{d}$ |
| RS (%) | 57.71 ± 0.56$^{a}$ | 45.61 ± 0.76$^{b}$ | 33.95 ± 0.58$^{c}$ | 28.85 ± 0.67$^{d}$ |

[a] DBNS and DENS represent starch nanoparticles, while DBS and DES represent native starch from *Dioscorea bulbifera* and *Dioscorea esculenta*, respectively. Data are expressed as mean ± the standard deviation. In each row, each value followed by a different superscript is significantly different ($P \leq 0.05$) as determined by Tukey's test.

of the sample particles to determine the mean hydrodynamic particle size.[68] Table 1 provides the mean hydrodynamic particle size, ZP, and PDI of raw and ball-milled DBS and DES. The mean particle size of DBS and DES reduced from 1019 nm and 1413 nm to 243 nm and 641 nm, respectively. The hydrodynamic size of the sample particles may appear bigger than the actual particle size because of particle swelling and surface charge of particles.[32] BM has been reported to fragment and reduce the size of starch extracted from water chestnut, lotus stem, horse chestnut,[28] pearl millet, proso millet, foxtail, sorghum,[32] and corn.[31] SNP with reduced particle size is promising as a reinforcement filler in food packaging.[69]

The PDI of DBS and DES decreased from 0.870 and 0.704 to 0.641 and 0.580, respectively. The reduction in PDI of DBNS and DENS shows that BM produced smaller particles with better dispersion and a narrow size distribution.[70] A similar reduction in PDI was observed during BM of starch extracted from pearl millet, proso millet,[32] and waxy corn.[66] The improved dispersion of nanofabricated starch enables promising use as fillers in edible packaging.[60]

**3.1.3. X-ray diffraction analysis.** The results of XRD analysis for raw and nano-reduced DBS and DES are shown in Fig. 4, which displays the Rietveld refined XRD images of raw and ball-milled DBS and DES with indexed peaks. The peaks in the XRD patterns are indexed with the Miller indices ($h$,$k$,$l$). DBS and DES exhibited a typical B-type pattern with crystalline and amorphous regions of starch. The prominent peaks at approximately 15°, 17°, and 23° indexed with Miller indices (1,2,0), (0,1,2), and (1,3,1), respectively represent a starch of B-type crystallinity. Hao *et al.*, reported B-type crystallinity with XRD peaks at 18° and 23° for starch.[65] Starch of B-type crystallinity features a hexagonal unit cell.[71] SI Fig. 5 shows the results of Rietveld refinement generated for raw and ball-milled DBS and DES by GSAS II software. The Rietveld refinement quality factor $R_{wp}$ (weighted profile $R$ factor) was 0.04167, 0.03754, 0.03849, and 0.05385 for DBS, DBNS, DES, and DENS, respectively. $R_{wp}$ value below 0.1 indicates high-quality refinement.[53] The Rietveld refinement of XRD of raw and ball-milled samples shows that the crystallinity of DBS and DES reduced with BM, as tabulated in Table 2. After Rietveld refinement, the apparent crystallite size of DBNS and DENS was found to be 3.8 nm and 3.38 nm,

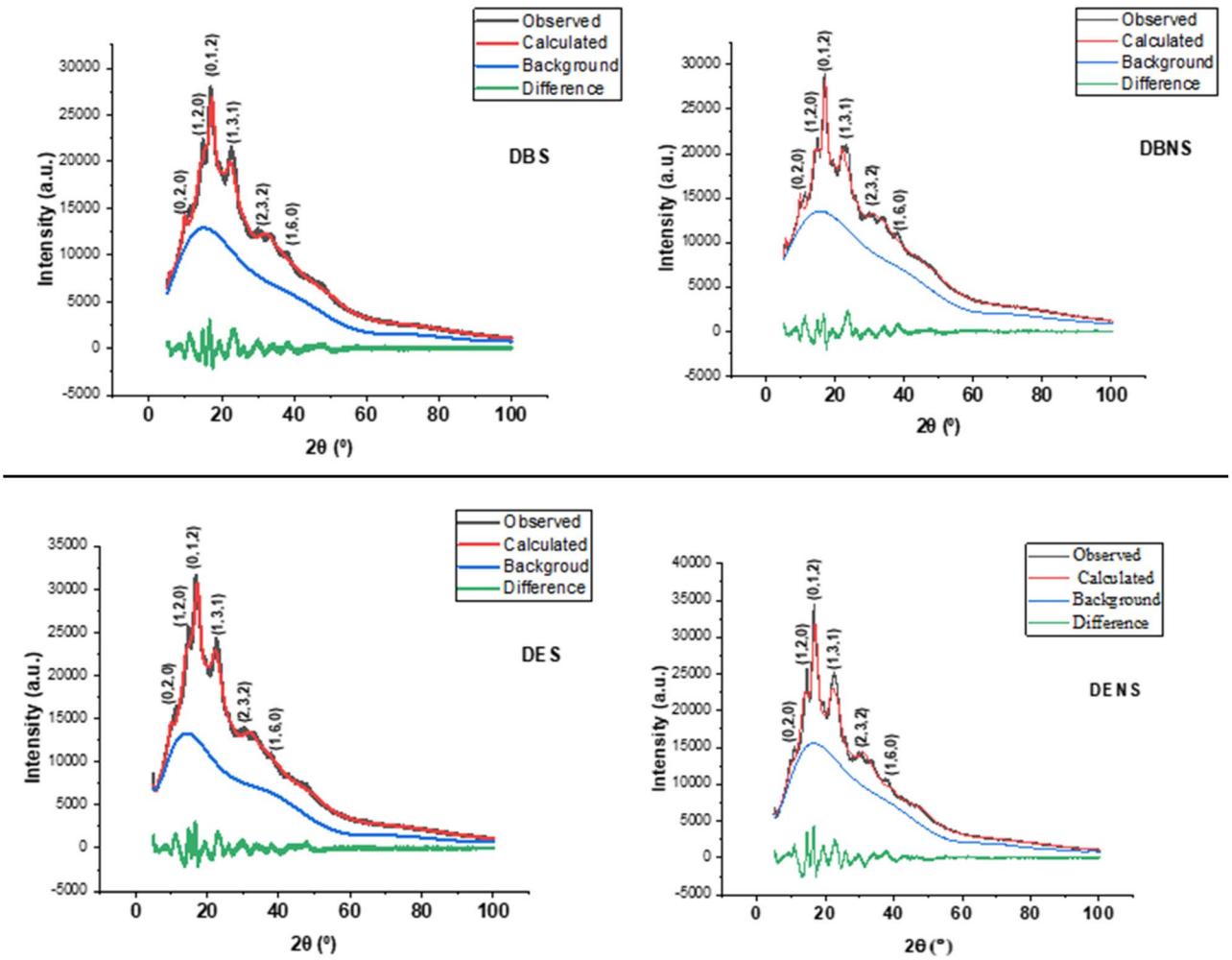


Fig. 4 Rietveld refined XRD spectra showing the effect of BM on raw *Dioscorea bulbifera* starch (DBS), and raw *Dioscorea esculenta* starch (DES). In the figure, the difference depicts the difference between the calculated values and observed values.

Table 2 Relative crystallinity, molecular order, FWHM of raw and ball-milled DBS and DES, quantified by XRD, FTIR, Raman spectroscopy, and % amorphous, % single helix, and % double helix conformations present in raw and ball-milled DBS and DES[a]

| Parameter | DBS | DBNS | DES | DENS |
|---|---|---|---|---|
| Crystallinity (%) | 37.0 | 30.75 | 42.29 | 28.5 |
| $R_{1047/1018}$ ($cm^{-1}$) | 0.650 | 0.627 | 0.582 | 0.577 |
| $R_{995/1018}$ ($cm^{-1}$) | 1.218 | 1.177 | 1.267 | 1.164 |
| FWHM at 480 $cm^{-1}$ | 20.72 | 38.77 | 20.39 | 29.36 |
| Amorphous (%) | 54.79 | 76.64 | 55.62 | 78.33 |
| Single helix (%) | 13.94 | 14.88 | 13.61 | 14.43 |
| Double helix (%) | 31.27 | 8.48 | 30.77 | 7.24 |

[a] DBNS and DENS represent starch nanoparticles, while DBS and DES represent native starch from *Dioscorea bulbifera* and *Dioscorea esculenta,* respectively. *R*: ratio of absorbance at wavenumbers 1047/1018 $cm^{-1}$ and 995/1018 $cm^{-1}$.

respectively. The crystallinity of starch depends on granule dimension, amylopectin content, interactions in the crystalline region, and double helix orientation. Crystallinity of starch is attributed to the three-dimensional structure of amylopectin. When subjected to BM, starch is disrupted, and amylopectin adopts a single-helical form, making it less crystalline.[72] The mechanical forces during BM distort the inherent configuration of starch. This process weakens the intermolecular and intramolecular bonds within starch.[65] The impact force, shear force, and collisions involved in BM generate mechanochemical modifications in starch that rupture glycosidic bonds and hydrogen bonds, and break down the crystalline portions of starch.[17] The amorphous nature of DBNS and DENS is directly associated with the increased amylose content due to BM. The increased amylose content reduces the scattering intensity for almost all diffraction peaks of DBNS and DENS.[72] BM was also reported to reduce the crystallinity of waxy maize starch,[73] pearl millet starch, proso millet starch,[32] and taro starch.[14] Barros *et al.*, reported that ball-milled cornstarch with reduced crystallinity formed a thin, brittle film without the incorporation of plasticizers.[31]

**3.1.4. Fourier transform infrared (FTIR) spectroscopy and Raman spectroscopy (RS).** The structural alterations induced by BM on DBS and DES were studied using FTIR spectroscopy. The interferogram is given in Fig. 5a. The unique bands of starch are generated because of the vibrations of amylose and amylopectin molecules. All the raw and nano-fabricated starch samples exhibited peaks at 3200–3300 $cm^{-1}$, because of the OH stretching in starch. The peak width denotes the total quantity of hydrogen bonds.[32] DBNS and DENS had a more intense FTIR band at 3296 $cm^{-1}$ than raw starch samples. From this, it can be inferred that the intermolecular hydrogen bonds of DBS and DES became stronger after BM.[66] This was due to the decrease in the size of DBS and DES following BM. The FTIR peak at 2932 $cm^{-1}$ denotes the asymmetric C–H vibration of $-CH_2-$. This vibration is affected by bound water molecules within starch.[66] The bands at 1147 and 1076 $cm^{-1}$ denote the C–C and O–H bond vibrations and asymmetric stretching of the glycosidic bond in starch.[28] The absorption bands at 1147 and 1076 $cm^{-1}$ represent the stretching of C–O and C–O–H anhydrous glucose rings within the starch molecule. The peaks near 990 $cm^{-1}$ correspond to the vibrations of α-1,4 glycoside bonds, which became less intense for DBNS and DENS, indicating that BM disintegrated glycosidic bonds of DBS and DES.[32] Juarez *et al.* observed that BM mechanolysed potato starch, cleaving the glycosidic bond of potato starch.[26] The alterations in the FTIR spectrum from 950 $cm^{-1}$ to 1050 $cm^{-1}$ of DBNS and DENS demonstrate that the shear, impact, and frictional forces of BM disrupted the crystalline portions of DBS and DES.[72] The FTIR peak at 1654 $cm^{-1}$, representing the scissoring vibrations of hydroxyl groups from hydration water on the non-crystalline

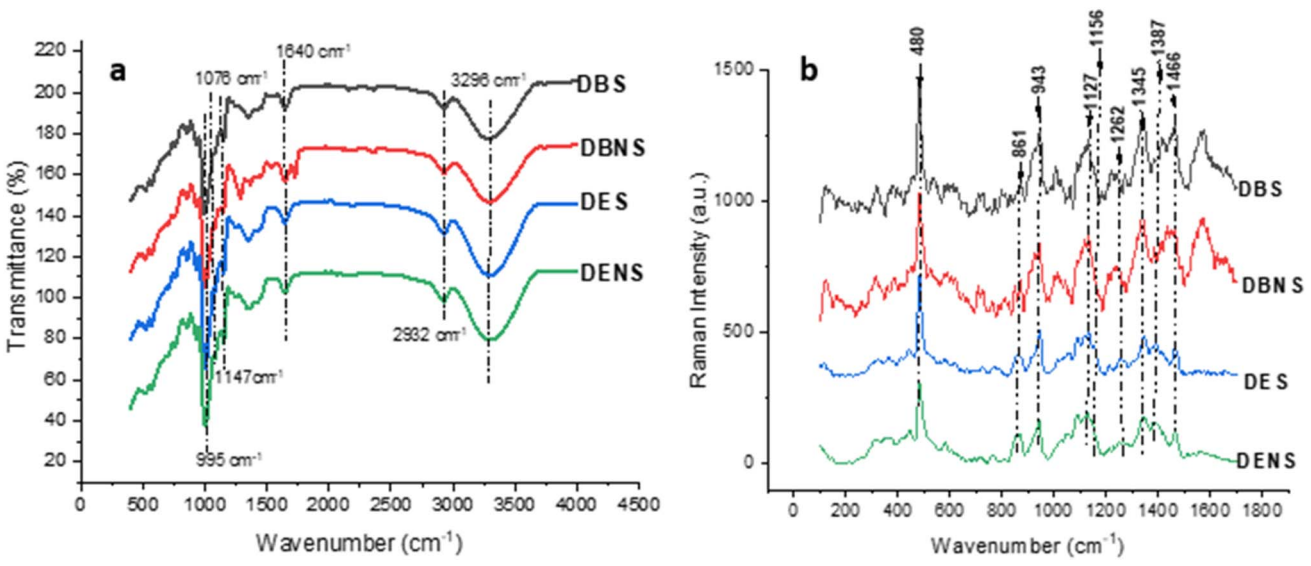


Fig. 5 (a) FTIR interferograms depicting the effect of BM on raw *Dioscorea bulbifera* starch (DBS) and raw *Dioscorea esculenta* starch (DES), (b) Raman spectra depicting the impact of BM on DBS and DES.

region of starch, increased for ball-milled samples due to an increase in the amorphous property.[66] The functional groups of raw and ball-milled DBS and DES showed minimal variation. Hence, BM is a promising physical technique for comminution of starch.[32] During the BM of DBS and DES, the kinetic energy from the collision between the ball, starch, and the ball milling equipment wall gets converted into mechanical forces such as shear and frictional forces. These mechanical forces selectively disrupt α-1,6 glycosidic bonds of amylopectin subunits within the starch molecules.[65]

Furthermore, during BM, the rotation of the balls within the BM equipment facilitates rapid particle movement, enabling thorough blending of the sample particles. The grinding action fragments larger sample particles and creates reactive contacts between sample particles. Then the impact force of the moving balls will activate the reactive contacts and thereby rupture the intermolecular hydrogen bonds within the sample molecules and thereby create sample deformation.[63]

In this research study, planetary ball milling equipment was used for the mechanochemical modification of DBS and DES. The planetary BM involves the combination of two distinct rotational motions. The BM jars rotate along the planetary axis, while concurrently rotating around their respective *Z*-axis, usually in the alternate direction. This counter rotation of the BM equipment produces substantial impact and shear forces upon the balls as they encounter the walls of the BM vessel. This brings about attrition of starch samples. Planetary BM energy is predominantly regulated by rpm and the running time of the BM.[74]

An increase in peak intensity of FTIR at 2932 $cm^{-1}$ of DBNS and DENS illustrates an increase in the disruption of intermolecular hydrogen bonds of amylopectin subunits of the starch molecule by the mechanical forces of BM. Kiymaz *et al.*, also observed a similar increase in the peak intensity of FTIR at 2943 $cm^{-1}$ for ball-milled taro starch, indicating the breakdown of the starch molecule by the mechanical forces of BM.[14] This fragmentation of starch (DBS & DES) due to BM is also seen in SEM and TEM images.

The absorbance ratio of FTIR signals on 995/1018 $cm^{-1}$ ($R_{995/1018}$), and 1047/1018 $cm^{-1}$ ($R_{1047/1018}$),[28,31] was used to determine the change in the crystalline structure of DBS and DES due to BM. There was a decrease in $R_{995/1018}$ and $R_{1047/1018}$ of DBS and DES after BM, as tabulated in Table 2. The result shows that BM disrupted the crystalline structure of starch after BM. The XRD measurements of the crystallinity index of DBNS and DENS aligned with these findings of FTIR. Ahmad *et al.*, reported a reduction in the absorbance ratio $R_{1047/1018}$ and $R_{995/1018}$ of starch extracted from horse chestnut, lotus stem, and water chestnut and after BM, depicting an increase in their amorphous nature.[28]

RS was used to investigate the alterations in the molecular structure of DBS and DES after BM. The Raman spectra of raw and nanoscale-fabricated DBS and DES are given in Fig. 5b. The RS image of nano-reduced DBS and DES exhibited similar bands, attributed to amylose and amylopectin.[72] RS images of raw and ball-milled DBS and DES show a complex set of vibrations at the wave number region below 800 $cm^{-1}$, revealing the vibrational motion of the pyranose ring in glucose. The Raman band at 480 $cm^{-1}$ serves as a marker for amylose and amylopectin in the samples. The Raman signal intensity at 480 $cm^{-1}$ for DBNS and DENS was less compared to DBS and DES. This reduced intensity indicates that BM disintegrated the ordered configuration of the starch matrix.[75] The spectral peak at 480 $cm^{-1}$ in the Raman spectra of the samples is responsive to the molecular arrangement of double helices within the starch molecules. The wavenumber shift can be due to external or internal influences on the starch bond length. BM decreased the Raman band intensity at 480 $cm^{-1}$ for DBNS and DENS, corresponding to the alterations in the particle size and crystallinity of DBS and DES. Kumar and Kumar also observed a similar reduction in the intensity of the 480 $cm^{-1}$ peak within the Raman spectra of ball-milled pink potato starch and ball-milled maize starch, denoting that BM resulted in an increase in its amorphous nature.[72]

The vibrational characteristics of starch, predominantly derived from glucose monomers, are depicted in the Raman spectra in the region 800 to 1500 $cm^{-1}$. These bands associated with skeletal vibrations of glucose units within starch underwent noticeable changes following BM.[72] The bands at 480, 861, 943, and 1127 $cm^{-1}$ represent C–C–O–, C1–O–C5, C–OH, and (C–O–H + C–OH) vibrational motion of the glucose pyranose ring, respectively. The Raman spectral bands at 480 $cm^{-1}$, 861 $cm^{-1}$, 943 $cm^{-1}$, and 1127 $cm^{-1}$ shifted to higher wavenumbers, which depict an alteration in the length of the glycosidic bond of DBS and DES because of BM.[72,76]

The prominent bands in the Raman spectra of DBNS and DENS, at wavenumbers from 900 to 960 $cm^{-1}$, associated with C–O–C of the α-1,4 and α-1,6 glycosidic bonds, exhibited remarkable alterations in the intensity, owing to the breakdown of α-1,6 glycosidic bonds of amylopectin subunits DBS and DES following BM. This increased the amorphous nature of DBS and DES.[72] The spectral bands of DBS and DES at 1262 $cm^{-1}$ and 1466 $cm^{-1}$ seem almost to disappear after BM, owing to the reductions in their crystallinity because of BM. These results agreed with the results of XRD analysis and FTIR analysis. Numerous studies reported that the FWHM of the 480 $cm^{-1}$ peak within the Raman spectra correlates with the overall length of the double helix.[72,77,78] The half-width of the Raman peak at 480 $cm^{-1}$ is directly associated with the starch crystallinity. The higher the FWHM, the higher the amorphous nature of starch.[65] The FWHM of DBS and DES increased upon BM, as shown in Table 2. This result shows that BM altered the structure of DBS and DES. Hao *et al.* reported a reduction in the FWHM at 480 $cm^{-1}$ for ball-milled high amylose corn starch ferulic acid complexes, denoting an increase in their crystallinity.[65]

**3.1.5. $^{13}C$ cross-polarization/magic angle spinning nuclear magnetic resonance (CP/MAS NMR) spectroscopy.** The $^{13}C$ CP/MAS NMR analysis was employed to study the helical conformations of raw and ball-milled DBS and DES, using potato starch (analytical grade) as the reference. Fig. 6 depicts the NMR spectra of DBS, DES, DBNS, and DENS. The NMR spectra of starch were grouped into four sections, depending upon the chemical shifts: $C_1$ (94 ppm to 105 ppm), $C_2$, $C_3$, $C_5$ (66 ppm to

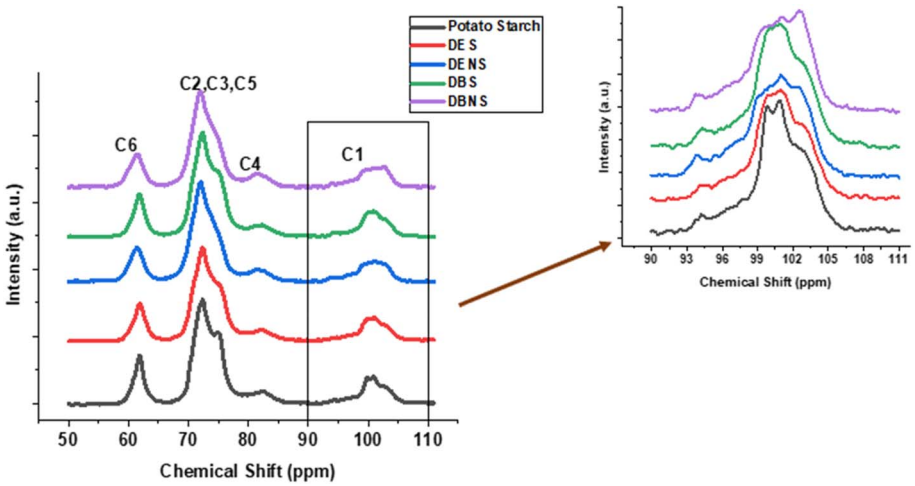


Fig. 6 $^{13}$C NMR spectrum showing the effect of BM on the structural properties of DBS and DES, taking potato starch as reference sample. Raw *Dioscorea bulbifera* starch (DBS), ball milled *Dioscorea bulbifera* starch (DBNS), raw *Dioscorea esculenta* starch (DES), and ball milled *Dioscorea esculenta* starch (DENS).

78 ppm), $C_4$ (80 ppm to 84 ppm), and $C_6$ (58 ppm to 65 ppm).[79] The alterations in the starch double helix corresponded to the $C_1$ peak intensity (Fig. 5). The $C_1$ signal (93–103 ppm) in $^{13}$C NMR of starch provides details about the amorphous and crystalline components of starch. The threefold symmetry of adjacent helices in B-type starch creates two equivalent residues. The $C_1$ part, on the other hand, has two peaks that overlap at roughly 103 and 101 ppm.[80] There were no remarkable differences observed in the $^{13}$C chemical shift among DBS, DES, DBNS, DENS, and potato starch. $C_1$ signals and $C_4$ signals in $^{13}$C NMR of starch denote ordered crystalline structure and amorphous structure within starch. $^{13}$C NMR of DBNS and DENS exhibited blurred $C_1$ signals, indicating disintegration of crystalline portions of DBS and DES due to the impact of BM.[80] The comparative amounts of amorphous portions, single helices, and double helices in raw and ball-milled starch samples after deconvolution of $C_1$ peaks (90–110 ppm) are given in Table 2. It was observed that the mechanical forces of BM enhanced the relative amounts of amorphous portions and led to a mild increase in the comparative amounts of single helices and a reduction in double helices. The kinetic energy of balls in BM disrupts the intermolecular hydrogen bonds and α-1,6 glycosidic bond within amylopectin subunits of starch, and thereby reduce the crystallinity of DBS and DES. Sun *et al.*, observed a reduction in the intensity of the $C_1$ peak and an enhancement in the intensity of the $C_4$ peak of waxy corn starch when subjected to BM and ultrasonication, depicting a reduction in crystallinity.[66] Zhang *et al.*, also observed an increase in the relative amount of the amorphous portion of ball-milled rice starch samples.[80]

These results are at par with the results of XRD analysis, FTIR absorbance ratios $R_{1047/1018}$ and $R_{995/1018}$ of nanofabricated DBS and DES, and FWHM at 480 cm$^{-1}$ of Raman spectroscopy, and denote a destruction of crystalline portions of DBS and DES following BM.

### 3.2. Evaluation of techno-functional properties of raw and nanoscale fabricated DBS and DES

**3.2.1. Colour analysis.** The colour analysis data of raw and ball-milled DBS and DES are tabulated in Table 1. Native starches DBS and DES, with higher $L^*$ values, and lesser $a^*$ and $b^*$ values, indicate their superior colour quality.[81] DBNS and DENS exhibited significantly lower ($P < 0.05$) $L^*$ and significantly higher ($P < 0.05$) $a^*$ and $b^*$ than DBS and DES, respectively. As a result of BM, amylopectin was disintegrated. These fragmented amylopectin forms complexes with various other small constituents found in the starch samples. These changes led to an increase in $a^*$ and $b^*$ of ball-milled DBS and DES.[32] Jhan *et al.*, observed a decrease in $L^*$ value and a rise in $a^*$ and $b^*$ values of ball-milled pearl millet starch and proso millet starch.[32] Dey and Sit, observed an improvement in $L$ value for foxtail millet starch modified using physical, chemical, and enzymatic methods.[82]

**3.2.2. Thermal analysis.** The DSC thermogram of DBS, DBNS, DES, and DENS is represented in the SI Fig. 6. The gelatinization temperatures of the samples ($T_o$, $T_p$, $T_c$) and gelatinization enthalpy ($\Delta H$) are tabulated in Table 1. The results of the DSC analysis indicated that the temperatures at which gelatinization occurred in DBNS and DENS were significantly ($p < 0.05$) lower than those of DBS and DES, respectively. BM makes DBS and DES less crystalline and more accessible to water.[31] This reduces the thermal gelatinization temperatures. In addition to that, the gelatinization enthalpy of DBNS and DENS was significantly ($P < 0.05$) lower than DBS and DES, respectively, because gelatinization of starch is influenced by the mean degree of polymerization (DP) of amylopectin within starch. BM reduces the DP of amylopectin in DBS and DES and makes double helical structures less stable, which in turn reduces the heat required for gelatinization.[83] The mechanical forces involved in the BM transform the double helical forms of raw DBS and DES into single helical forms. This transformation increases the susceptibility of DBNS and DENS to melting,

thereby reducing their gelatinization enthalpy.[32] The relative amounts of the crystalline portion of starch constitute an essential factor in determining the thermal stability of starch.[66]

Earlier studies reported that BM reduced the thermal stability of waxy corn starch,[66] sorghum starch, foxtail millet starch,[33] and corn starch.[31] The reduction in the crystallinity of starch by BM enhances the accessibility of water to starch, which facilitates the starch gelatinization at a lower temperature than raw starch. Hence, less energy will be needed to gelatinize nano-reduced amorphous starch.[31] The ball-milled corn starch with reduced gelatinization temperatures was reported to form thin and brittle films without the incorporation of plasticizers.[31]

**3.2.3. Apparent amylose content.** The Apparent Amylose Content (AAC) of DBS, DES, DBNS, and DENS is tabulated in Table 1. DBS and DES had an apparent amylose content of 17.75 ± 0.58% and 9.54 ± 0.50%, respectively. Previous studies have reported an average amylose content of 19.53% and 9.73% for DBS and DES, respectively.[44] Amylose content depends upon the source, structure, and starch extraction methods.[33] There was a significant rise ($P < 0.05$) in the AAC of DBS and DES following BM, as shown in Table 1. The mechanical forces of BM disintegrate α-1,6 glycosidic linkages of branched amylopectin of DBS as well as DES and thereby convert it to amylose.[65]

A similar increase in amylose content was reported for ball-milled wheat starch,[64] high amylose corn starch,[65,84] foxtail millet starch, and sorghum starch.[33] In the current study, DBNS exhibited a significantly ($P < 0.05$) higher apparent amylose content compared to DENS, which may be attributed to the smaller APS of DBNS, as observed in the results of TEM and zeta analysis. The higher amylose content in the nano-reduced starch enhances its film-forming capacity.[85] Hence, DBNS and DENS can be used in edible packaging applications.

**3.2.4. Rheology evaluation.** The rheological properties of starches are crucial in the food industry because of their thickening nature.[86] Fig. 7 depicts the rheological properties of raw and ball-milled DBS and DES. The storage modulus denotes the energy retained by the starch gel during deformation, and the loss modulus is the energy dissipated to overcome viscous force.[87] The plot of the storage modulus ($G'$) and loss modulus ($G''$) of DBS, DES, DBNS, and DBNS *versus* angular frequency is given in Fig. 7a. $G'$ of all the samples was predominant over $G''$, throughout the frequency sweep test, implying the elastic property of starch.[32] The greater magnitude of $G'$ than $G''$ indicates weak gel rheology, characteristic of pseudoplastic fluids, demonstrating enhanced viscoelasticity of the gel.[88] The $G'$ values of gels of raw as well as ball-milled DBS and DES were consistently greater than $G''$, indicating starch gels remained viscoelastic fluid.[60] DBNS and DENS exhibited enhanced viscoelastic properties compared to DBS and DES. They exhibited strong gel behavior upon slight deformation, but the starch network degraded as strain increased. The mechanical forces

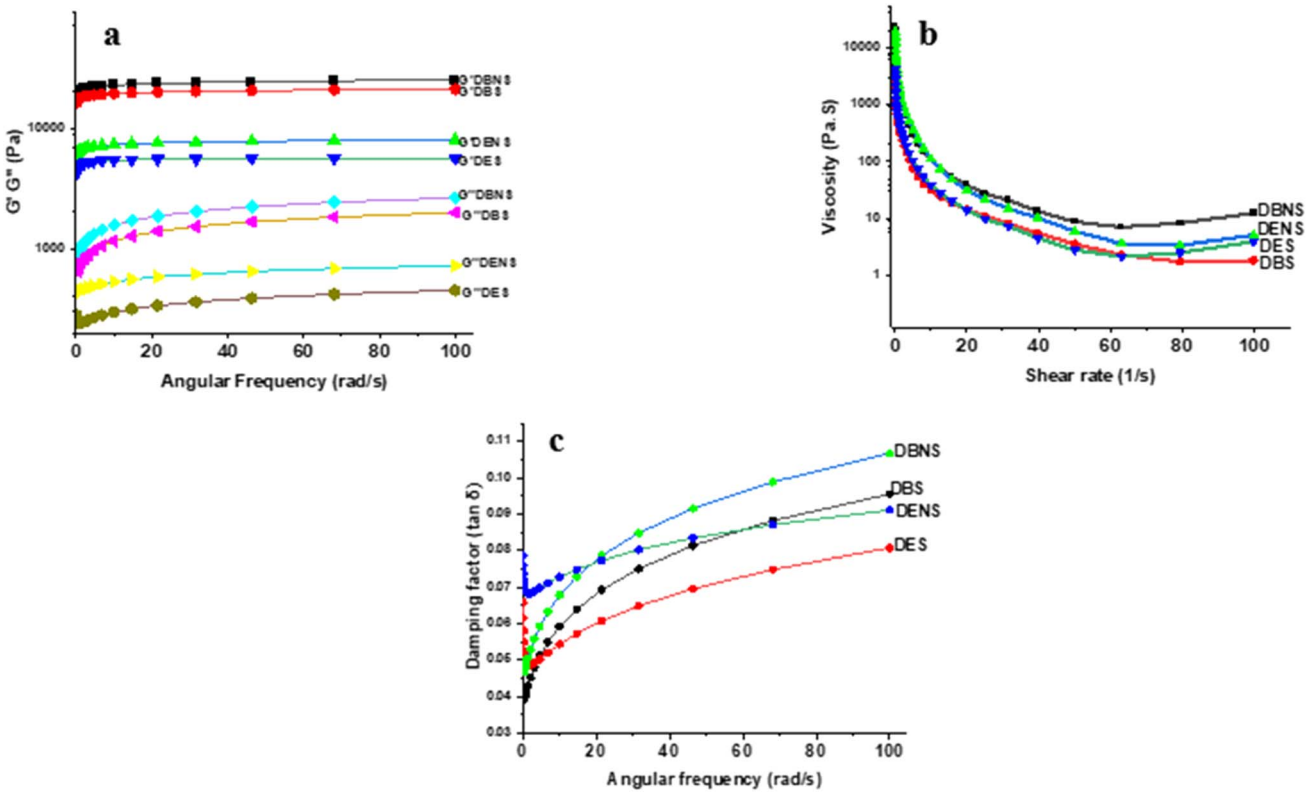


Fig. 7 Rheological evaluation results depicting the effect of BM on storage modulus, loss modulus, damping factor, and viscosity of DBS and DES. (a) Storage modulus $G'$ and loss modulus $G''$ of ball-milled DBS and DES in comparison with raw DBS and DES against the frequency sweep, (b) viscosity of raw and ball-milled DBS and DES against shear rate (0.01–100 $s^{-1}$), and (c) damping factor of raw and ball-milled DBS and DES against angular frequency.

during BM transform the structure of starch and thereby enhance the viscoelasticity of DBNS and DENS (Fig. 7b).[32] When DBS and DES were subjected to BM, the impact, shear, and frictional forces developed because of the collision between starch, balls, and walls of the BM vessel, disrupting the intermolecular hydrogen bonds of amylopectin subunits of starch. This makes the starch amorphous, and this enables the starch chain mobility, improving the accessibility of the starch to water. This, in turn, reduces the gelatinization temperature of starch. Hence, the viscosity of starch increases. During hydration, the amorphous regions of starch swell with greater ease, which enables increased polymer chain fragmentation and positioning upon the application of shear force. This enhances the viscosity and storage modulus of starch.[31] Furthermore, DBNS exhibited improved viscoelasticity compared to DENS, which might be owing to the smaller APS of DBNS. Jhan *et al.*, reported that nano-reduced millet starches exhibited enhanced viscoelastic properties than raw millet starches.[32] Ahmad *et al.*, reported that nano-reduced water chestnut, horse chestnut, and lotus stem starches exhibited improved viscoelasticity than their raw counterparts.[28] DBNS and DENS had higher viscosity than DBS and DES, respectively, as depicted in Fig. 6b. This improved viscoelasticity of DBNS and DENS was due to the size reduction and changes in molecular interactions of DBS and DENS induced by ball-milling. The rheology of starch depends upon its morphology, amylose content, and molecular interaction.[28]

Nanoscale fabricated starch suspensions prepared from corn and cassava starch were also reported to have greater viscosity than their raw starches.[89,90] The viscosity of all the samples reduces with increasing shear rate, as seen in Fig. 6b. The orientation of starch molecules changed upon the application of stress; hence, their viscosity became stable. This experiment demonstrated shear thinning behavior of the samples. The mechanical forces of BM disintegrated the molecular arrangement of starch, which in turn decreased the entangling points in the starch gel. Hence, the starch gel is susceptible to destruction, which leads to lower viscosity.[87]

The damping factor represents how a system behaves physically by depicting the ratio of viscous to elastic sections of viscoelastic deformation. Gels of DBNS and DENS exhibited a higher damping factor than DBS and DES (Fig. 7c). For starch gels with a damping factor (tan $\delta$) less than 1, the elastic characteristics dominate the viscous characteristics of the gel.[91] Starch gels with a greater damping factor tend to be more viscous, less rigid, less elastic, and simpler to process. This contributes to the commercial application of starch as fillers and thickeners.[92] Wang *et al.* documented that acrylic acid–methyl acrylate modified starch with enhanced viscoelasticity was able to form films with improved flexibility.[93] Hence, DBNS and DENS with enhanced viscoelasticity can be used to fabricate flexible edible packaging.

**3.2.5. Water and oil absorption capacity.** WAC and OAC of starch represent the potential of starch to absorb and hold water/oil under specific conditions. WAC and OAC of the raw and nanoscale fabricated DBS and DES are given in Table 1. The WAC of DBS and DES significantly ($p < 0.05$) increased upon nano-reduction. Ahmad *et al.* reported that BM significantly ($P < 0.05$) improved the WAC of starch extracted from horse chestnut starch, lotus stem, and water chestnut starch.[28] Chen *et al.* also observed that the WAC of quinoa starch increased as the starch became amorphous due to the BM.[94] Higher WAC of nano-reduced starch might be owing to the greater surface area and vulnerability of hydrophilic granular regions of the sample. WAC depends on the relative amount of amorphous, crystalline regions and hydrophilic groups present in the starch.[95] BM breaks the amylose and amylopectin chains of starch, thereby exposing amylose regions of starch that possess multiple water-binding sites.[31]

The OAC of DBS significantly ($p < 0.05$) increased with BM, as tabulated in Table 1. Kiymaz *et al.* reported an improvement in the OAC of taro starch after BM. Capillary force is the physical basis for the binding of oil onto starch.[14] This significant increase in the OAC resulted from the enhanced surface area of DBS and DES, which resulted in the formation of a steric hindrance across the oil interface.[66] Sun *et al.* also observed an enhancement of OAC of waxy corn starch after BM.[66]

The higher WAC of starch nanoparticles renders them appropriate for manufacturing food packaging that prevents moisture loss and effectively prolongs food shelf-life.[96] Sharma *et al.* found that the OAC of the kidney bean SNP was significantly ($P < 0.05$) greater than raw starch.[97] The higher OAC of nanostarch will be beneficial for the retention of flavor and essential oils.[97] Therefore, DBNS and DENS can be used to encapsulate flavor and essential oils.

**3.2.6. Evaluation of digestive properties.** The results of the digestibility study of raw and ball-milled DBS and DES are given in Table 1. BM significantly increased ($P < 0.05$) RDS and significantly decreased ($P < 0.05$) SDS and RS of DBS and DES. The SPSS Box plot for Rapidly Digestible Starch (RDS), Slowly Digestible Starch (SDS), and Resistant Starch (RS) is given in SI Fig. 7. BM greatly improves the enzymolysis of starch during *in vitro* digestion.[64] BM impaired the starch bonds, thereby transforming a portion of SDS and RS to RDS. The *in vitro* digestion of starch depended greatly on the interaction and binding capacity of amylase and glucoamylase with starch.[98] The mechanolysis of starch by BM enhanced the surface area of DBS and DES. This enhanced the contact area of DBS and DES for the enzymolysis by amylase during *in vitro* digestion. This facilitates the formation of increased quantities of RDS.[99] The damage to the helical structure of starch by BM affects the pace of *in vitro* digestion of starch samples.[64] The mechanical forces during BM decrease the crystallinity of starch and enhance the digestibility of starch, thereby improving the utility of starch.[17]

During *in vitro* digestion, amylase and glucoamylase break down the $\alpha$-1,4 glycosidic linkages present within starch. Starch digestion comprises three steps. First, the movement of amylase and glucoamylase to starch (substrate), then the formation of enzyme–substrate complexes, and finally the hydrolysis of the glycosidic linkages.[64] The efficiency of starch digestion by enzymes depends on the surface characteristics and crystallinity of starch molecules. BM generated cracks in *Dioscorea bulbifera* starch and *Dioscorea esculenta* starch, as revealed by SEM and TEM. This facilitates the easier penetration of the

 

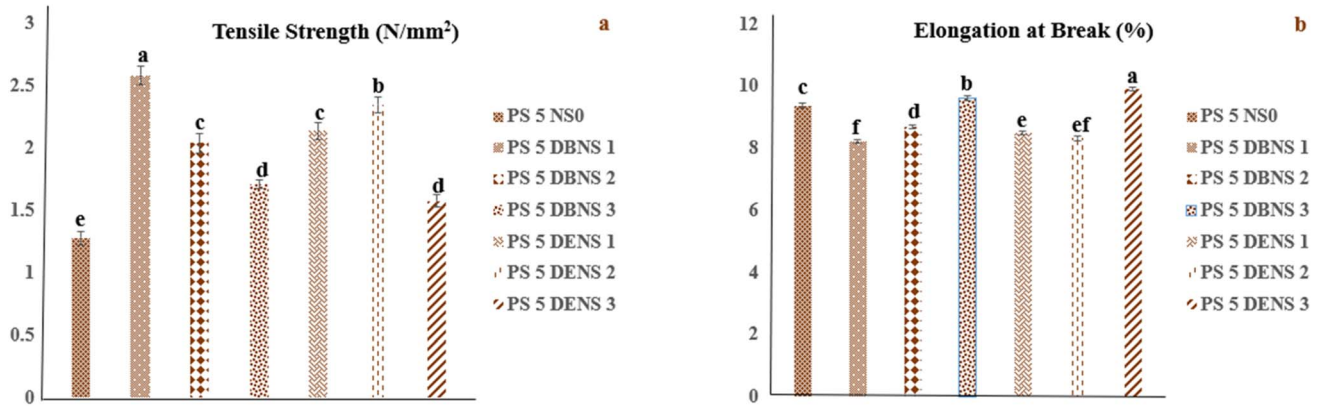


Fig. 8 Results of (a) tensile strength, and (b) elongation at break evaluation of starch-based edible film made from 5% w/w/potato starch (PS) and glycerol (30% w/w of starch) incorporated with different concentrations of DBNS (1, 2, and 3% w/w), and DENS (1, 2, and 3% w/w).

enzyme into starch during its *in vitro* digestion. In short, BM increased the void index of the glucan chains in starch molecules, facilitating faster amylase action on starch.[64] Previous studies reported that BM increased the digestibility of wheat starch,[64] and foxtail millet flour.[36] The enhanced digestibility of DBNS and DENS makes them appropriate candidates to manufacture edible films that are eaten with the food.[100]

### 3.3. Application study of DBNS and DENS in potato starch-based edible films and characterization of its mechanical properties

The results of testing the tensile strength and elongation at break of the prepared edible films are given in Fig. 8. The incorporation of DBNS and DENS (up to 1% w/w and 2% w/w, respectively) in potato starch-based edible film significantly ($p < 0.05$) enhanced the tensile strength and reduced the elongation at break of potato starch-based edible film. DBNS and DENS are predicted to have interactions with –OH groups or van der Waals bonds of potato starch, hence enhancing the molecular interactions between potato starch and starch nanoparticles.[9] The incorporation of 2% w/w DBNS, 3% w/w DBNS, and 3% DENS, respectively, was found to reduce the tensile strength and increase the elongation at break of the potato starch-based edible films. The reduction in tensile strength of starch-based edible film is associated with the accumulation of starch nanoparticles within the film.[9]

## 4. Conclusion

A green technique, such as wet BM, was used for the nanoscale fabrication of starch from two underutilized yams, *Dioscorea bulbifera* and *Dioscorea esculenta*, to address consumer demand for natural and eco-friendly starch modification techniques. The techno-functional attributes were employed as evaluation indices to study the impact of nanoscale fabrication on DBS and DES, assess the processing adaptability of DBNS and DENS, and broaden their application avenues in flexible edible packaging. Starch nanoparticles with enhanced dispersibility were successfully prepared using wet BM. The smaller size and better dispersibility enable them to be used as reinforcement filler in flexible edible food packaging. The incorporation of DBNS/DENS into potato starch-based edible films improved the flexibility of the potato starch-based edible films. The mechanical forces involved in the nanoscale fabrication resulted in the formation of fractured DBNS and DENS with rougher surfaces, as depicted by the results of SEM and TEM analysis. BM disrupted DBS and DES as implied by the increase in FTIR peak intensity at 2932 $cm^{-1}$ and reduction in the Raman band intensity at 480 $cm^{-1}$ of DBNS and DENS. The nanoscale fabrication increased AAC and reduced the gelatinization enthalpy of DBS and DES, which can potentially improve their film-forming capacity. Rheology evaluation revealed that nanoscale fabrication improved the viscoelasticity of DBS and DES, making them promising materials in the preparation of flexible edible films. Nanoscale fabrication significantly improved the RDS, WAC, and OAC of both DBS and DES. The enhanced dispersibility, viscoelasticity, digestibility, and reduced gelatinization enthalpy of DBNS and DENS may improve their effectiveness as fillers as well as packaging material in flexible edible food packaging. The enhanced dispersibility, viscoelasticity, digestibility, and reduced gelatinization enthalpy of DBNS and DENS validated the hypothesis of this study. Further, the DBNS and DENS need to be incorporated into edible films and extensively assessed under real-time storage conditions for their effectiveness in altering the barrier, thermal, biodegradable, and digestible properties to confirm their practical applicability. At present, the use of starch in the fabrication of edible packaging is constrained by its low moisture–barrier properties. The starch nanoparticles derived from underutilized *Dioscorea* species may be employed as fillers in edible packaging to enhance flexibility, oxygen barrier capacity, and moisture resistance due to enhanced techno-functional attributes. Furthermore, these starch nanoparticles may be used to deliver antimicrobial and antioxidant agents, thereby prolonging the shelf life of dairy, perishable, and minimally processed foods.

Additional studies are recommended to evaluate the economic feasibility and process optimization required for

commercial-scale ball milling. Further research is necessary to address the regulatory compliance for the safe and large-scale applications of these materials in edible packaging.

## Conflicts of interest

The authors declare no conflict of interest.

## Data availability

The data supporting this article have been included as part of the supplementary information (SI). Supplementary information is available. See DOI: https://doi.org/10.1039/d6ra00319b.

## Acknowledgements

The authors acknowledge SRM Central Instrumentation Facility, SRM Institute of Science and Technology, Nanotechnology Research Centre, SRM Institute of Science and Technology, and School of Bioengineering, SRM Institute of Science and Technology (SRMIST) for providing analysis facilities. We express our thanks to Prof. C. Muthamizchelvan, V. C., SRM Institute of Science and Technology, Dr Leenus Jesu Martin M, Dean, Faculty of Engineering and Technology and Dr Parani M, Chairperson, School of Bioengineering, SRM Institute of Science and Technology, for cordial support. We also extend our gratitude to the Sophisticated Analysis Instrumentation Facility and the Center for Soft and Biological Matter, Indian Institute of Technology, Madras, for providing the analysis facilities.

## References

1 A. K. Singh, M. Lee, D. Jang and Y. S. Lee, *Trends Food Sci. Technol.*, 2024, **143**, 104273.
2 N. Pooja, I. Chakraborty, M. H. Rahman and N. Mazumder, *3 Biotech*, 2023, **13**, 220.
3 B. Elyasi Far, Y. Ahmadi, A. Yari Khosroshahi and A. Dilmaghani, *Adv. Pharm. Bull.*, 2020, **10**, 350–358.
4 T. Jiang, Q. Duan, J. Zhu, H. Liu and L. Yu, *Adv. Ind. Eng. Polym. Res.*, 2020, **3**, 8–18.
5 A. Karnwal, A. Rauf, A. Y. Jassim, M. Selvaraj, A. R. M. S. Al-Tawaha, P. Kashyap, D. Kumar and T. Malik, *Food Chem.: X*, 2025, **29**, 102662.
6 A. Apriyanto, J. Compart and J. Fettke, *Plant Sci.*, 2022, **318**, 111223.
7 H. Marta, D. I. Rizki, E. Mardawati, M. Djali, M. Mohammad and Y. Cahyana, *Polymers*, 2023, **15**, 1167.
8 E. Ojogbo, E. O. Ogunsona and T. H. Mekonnen, *Mater. Today Sustain.*, 2020, **7–8**, 100028.
9 A. N. Ahmad, S. A. Lim, N. Navaranjan, Y.-I. Hsu and H. Uyama, *Polymer*, 2020, **202**, 122646.
10 Q. Yang, X. Hu, Q. Bao, Y. Zhao, S. Zhang, S. Li and T. Li, *LWT-Food Sci. Technol.*, 2023, **185**, 115138.
11 C. Qiu, C. Wang, C. Gong, D. J. McClements, Z. Jin and J. Wang, *Int. J. Biol. Macromol.*, 2020, **152**, 117–125.
12 H. Nawaz, R. Waheed, M. Nawaz and D. Shahwar, in *Chemical Properties of Starch*, IntechOpen, 2020.
13 J. Compart, A. Singh, J. Fettke and A. Apriyanto, *Polymers*, 2023, **15**, 3491.
14 B. M. Kiymaz, D. Ozmen, A. Moin, B. Çiçek, O. S. Toker and M. Arici, *Int. J. Biol. Macromol.*, 2025, **321**, 146300.
15 L. M. Fonseca, S. L. M. El Halal, A. R. G. Dias and E. d. R. Zavareze, *Carbohydr. Polym.*, 2021, **274**, 118665.
16 S. Punia, *Int. J. Biol. Macromol.*, 2020, **144**, 578–585.
17 S. P. Bangar, A. Singh, A. O. Ashogbon and H. Bobade, *Int. J. Biol. Macromol.*, 2023, **237**, 124069.
18 F. G. Torres and G. E. De-la-Torre, *Int. J. Biol. Macromol.*, 2022, **194**, 289–305.
19 S.-J. Ye and M.-Y. Baik, *Food Sci. Biotechnol.*, 2023, **32**, 875–883.
20 C. Qiu, Y. Hu, Z. Jin, D. J. McClements, Y. Qin, X. Xu and J. Wang, *Trends Food Sci. Technol.*, 2019, **92**, 138–151.
21 R. Chang, N. Ji, M. Li, L. Qiu, C. Sun, X. Bian, H. Qiu, L. Xiong and Q. Sun, *Ultrason. Sonochem.*, 2019, **58**, 104660.
22 Q. Lin, Y. Liu, L. Zhou, N. Ji, L. Xiong and Q. Sun, *Food Hydrocoll.*, 2022, **127**, 107513.
23 V. Sreejit, R. Preetha, S. A. Mubeena and S. Dhananjay, *J. Nanopart. Res.*, 2025, **27**, 105.
24 C. R. Guimarães, A. F. Monteiro, D. O. Fasheun, W. B. Monteiro, A. S. da Silva, E. P. S. Bon, R. S. S. Teixeira and V. S. Ferreira-Leitão, *Bioenergy Res.*, 2025, **18**, 55.
25 X. Tian, Z. Wang, X. Wang, S. Ma, B. Sun and F. Wang, *Int. J. Biol. Macromol.*, 2022, **206**, 306–312.
26 E. A. Juarez-Arellano, M. Urzua-Valenzuela, M. A. Peña-Rico, A. Aparicio-Saguilan, M. Valera-Zaragoza, A. A. Huerta-Heredia and A. K. Navarro-Mtz, *Food Res. Int.*, 2021, **140**, 109870.
27 G. Gorrasi and A. Sorrentino, *Green Chem.*, 2015, **17**, 2610–2625.
28 M. Ahmad, A. Gani, F. A. Masoodi and S. H. Rizvi, *Int. J. Biol. Macromol.*, 2020, **151**, 85–91.
29 W. A. Ali, S. E. Richards and R. H. Alzard, *J. Ind. Eng. Chem.*, 2025, **149**, 63–93.
30 L. C. González, M. A. Loubes, M. M. Bertotto, R. I. Baeza and M. P. Tolaba, *Carbohydr. Polym. Technol. Appl.*, 2021, **2**, 100168.
31 M. de Oliveira Barros, A. L. A. Mattos, J. S. de Almeida, M. de Freitas Rosa and E. S. de Brito, *Foods*, 2023, **12**, 2924.
32 F. Jhan, A. Shah, A. Gani, M. Ahmad and N. Noor, *Int. J. Biol. Macromol.*, 2020, **159**, 1113–1121.
33 F. Jhan, A. Gani, N. Noor, Z. ul Ashraf, A. Gani and A. Shah, *Sci. Rep.*, 2021, **11**, 4873.
34 J. Joy, A. Krishnamoorthy, A. Tanna, V. Kamathe, R. Nagar and S. Srinivasan, *Appl. Sci.*, 2022, **12**, 9312.
35 X. Li, M. Fan, Q. Huang, S. Zhao, S. Xiong, B. Zhang and T. Yin, *Food Hydrocoll.*, 2020, **109**, 106082.
36 L. Yang, Y. Wang, P. Li, J. Weng, W. Zhao, Y. Jia and J. Liu, *Food Chem.*, 2025, **486**, 144554.
37 J. L. Howard, Q. Cao and D. L. Browne, *Chem. Sci.*, 2018, **9**, 3080–3094.
38 P. A. Magallanes-Cruz, L. F. Duque-Buitrago and N. del Rocío Martínez-Ruiz, *Food Res. Int.*, 2023, **169**, 112875.

39 D. Knorr and M. A. Augustin, *J. Sci. Food Agric.*, 2025, **105**, 735–746.
40 S. Kashyap, P. P., B. A. Dodke, A. G. Moon, S. Bagade, S. Tadas, S. Bhagat and S. Ansari, *Int. J. Pharm. Pharm. Res.*, 2018, **12**, 357–368.
41 M. Sahoo, S. Titikshya, V. Kumar and S. N. Naik, *Food Biosci.*, 2023, **56**, 103103.
42 E. Pérez, A. Ciarfella and M. B. Raymúndez B, *Acta Microsc.*, 2016, **25**, 16–20.
43 S. Rickett, L. A. Louderback and A. V. Bell, *Plants*, 2025, **14**, 1869.
44 E. Afoakwa, D. Polycarp, A. Budu, H. Mensah-Brown and E. Otoo, *Afr. J. Food, Agric., Nutr. Dev.*, 2013, **13**, 8106–8127.
45 J. Li, Y. Yue, Z. Lu, Z. Hu, Y. Tong, L. Yang, G. Ji and P. Liu, *Int. J. Biol. Macromol.*, 2024, **277**, 134552.
46 M. E. Rodriguez-Garcia, M. A. Hernandez-Landaverde, J. M. Delgado, C. F. Ramirez-Gutierrez, M. Ramirez-Cardona, B. M. Millan-Malo and S. M. Londoño-Restrepo, *Curr. Opin. Food Sci.*, 2021, **37**, 107–111.
47 W. D. R. Pokatong and J. Decyree, *Reaktor*, 2019, **18**, 224–234.
48 H. Chen, Z. Hu, D. Liu, C. Li and S. Liu, *Molecules*, 2019, **24**, 2973.
49 W. Zhang, W. Ding, K. H. Ndeurumi, Z. Wang and Y. Feng, *Starch/Staerke*, 2015, **67**, 958–963.
50 K. Harini, K. Ramya and M. Sukumar, *Carbohydr. Polym.*, 2018, **201**, 329–339.
51 M. J. Maria, R. Preetha and V. Sreejit, *Int. J. Food Sci. Technol.*, 2024, **59**, 2033–2041.
52 R. Shruthy and R. Preetha, *ACS Agric. Sci. Technol.*, 2024, **4**, 1216–1229.
53 C. da Costa Pinto, E. A. Sanches, M. T. Pedrosa Silva Clerici, M. T. Pereira, P. H. Campelo and S. Michielon de Souza, *Food Hydrocoll.*, 2021, **117**, 106682.
54 C. C. Pinto, P. H. Campelo and S. Michielon de Souza, *J. Appl. Polym. Sci.*, 2020, **137**(47), 49529.
55 R. Shruthy and R. Preetha, *Appl. Nanosci.*, 2022, **12**, 295–307.
56 R. Shruthy and R. Preetha, *Appl. Surf. Sci.*, 2019, **484**, 1274–1281.
57 X. Lin, S. Sun, B. Wang, B. Zheng and Z. Guo, *Int. J. Biol. Macromol.*, 2020, **157**, 240–246.
58 T. Tamilselvan, M. Saravanan and P. Prabhasankar, *Innovative Food Sci. Emerging Technol.*, 2024, **98**, 103860.
59 A. F. C. Algar, A. B. Umali, R. Rodrigo and P. Tayobong, *J. Microbiol., Biotechnol. Food Sci.*, 2019, **9**, 34–37.
60 Y. Wang, K. Di, Y. Sun, X. Li, J. Zheng and F. Zhang, *Foods*, 2025, **14**, 208.
61 K. Englyst, A. Goux, A. Meynier, M. Quigley, H. Englyst, O. Brack and S. Vinoy, *Food Chem.*, 2018, **245**, 1183–1189.
62 S. Rajagopal, V. Sreejit and R. Preetha, *J. Food Sci. Technol.*, 2025, **62**, 1689–1700.
63 C. Sun, K. Du, Z. He, Z. Zhu, Y. Hu, C. Wang, L. Mei, Q. Xie, Y. Chen, Y. Liu, G. Luo, S. Mustafa, X. Chen and X. Du, *Food Chem.*, 2025, **463**, 141148.
64 N. Han, J.-L. Fan, N. Chen and H.-Q. Chen, *J. Cereal Sci.*, 2022, **104**, 103439.
65 Z. Hao, S. Han, Z. Zhao, Z. Wu, H. Xu, C. Li, M. Zheng, Y. Zhou, Y. Du and Z. Yu, *Food Chem.: X*, 2024, **24**, 101919.
66 C. Sun, Y. Hu, Z. Zhu, Z. He, L. Mei, C. Wang, Q. Xie, X. Chen and X. Du, *Int. J. Biol. Macromol.*, 2024, **272**, 132862.
67 H. Lin, L. Z. Qin, H. Hong and Q. Li, *J. Nano Res.*, 2016, **40**, 174–179.
68 M. E. A. Mohsin, A. F. A. Rahman, Z. Harun, A. Arsad, S. Mousa, M. A. Ahmad Zaini, M. Y. Younes and M. F. Khan, *Polymers*, 2025, **17**, 1071.
69 E. P. Bhavya and M. Raman, *J. Packag. Technol. Res.*, 2024, **8**, 153–166.
70 J. Wang, Y.-D. Yu, Z.-G. Zhang, W.-C. Wu, P.-L. Sun, M. Cai and K. Yang, *Front. Bioeng. Biotechnol.*, 2022, **10**, 986033.
71 K. Dome, E. Podgorbunskikh, A. Bychkov and O. Lomovsky, *Polymers*, 2020, **12**, 641.
72 R. Kumar and K. J. Kumar, *Int. J. Biol. Macromol.*, 2024, **273**, 132900.
73 L. Dai, C. Li, J. Zhang and F. Cheng, *Carbohydr. Polym.*, 2018, **180**, 122–127.
74 G. Yang, Y. Jaberi, E. Lam and A. Moores, *Green Chem.*, 2026, **28**, 3006–3042.
75 K. Kaczmarska, B. Grabowska, T. Spychaj, M. Zdanowicz, M. Sitarz, A. Bobrowski and S. Cukrowicz, *Spectrochim. Acta, Part A*, 2018, **199**, 387–393.
76 A. Martinez-Garcia, L. Fink, L. Bayarjargal, B. Winkler, E. A. Juarez-Arellano and A. K. Navarro-Mtz, *Int. J. Biol. Macromol.*, 2024, **260**, 129579.
77 S. Yang, S. Dhital, C.-S. Shan, M.-N. Zhang and Z.-G. Chen, *Carbohydr. Polym.*, 2021, **270**, 118367.
78 Y. Wang, C. Chao, H. Huang, S. Wang, S. Wang, S. Wang and L. Copeland, *J. Agric. Food Chem.*, 2019, **67**, 8212–8226.
79 S. Han, Z. Wu, Z. Zhao, H. Xu, J. Hu, Y. Xiao, Y. Liu, K. Liu, Y. Wang, S. Li, M. Zheng, Y. Zhou, Y. Du and Z. Yu, *LWT-Food Sci. Technol.*, 2024, **212**, 116969.
80 B. Zhang, Z. Yuan, D. Qiao, S. Zhao, Q. Lin and F. Xie, *ACS Food Sci. Technol.*, 2021, **1**, 636–643.
81 F. Wang, M. Xu, Y. Jiang, B. Zhang, Y. Shao, J. Liu, J. Kan, M. Zhang, L. Xiao, X. Qi, L. Li, S. Zhao and C. Qian, *Horticulturae*, 2024, **10**, 1200.
82 A. Dey and N. Sit, *Int. J. Biol. Macromol.*, 2017, **95**, 314–320.
83 Y. Tian, J. Li, M. Nie, L. Wang, L. Liu, F. Wang and L.-T. Tong, *Food Chem.: X*, 2025, **27**, 102423.
84 Y. Ding, J. Zheng, X. Xia, T. Ren and J. Kan, *Carbohydr. Polym.*, 2016, **141**, 151–159.
85 F. Zhu, *Food Res. Int.*, 2025, **204**, 115758.
86 S. J. Yoon, J. Bak and B. Yoo, *Int. J. Biol. Macromol.*, 2024, **264**, 130600.
87 L. Chen, Y. Dai, H. Hou, W. Wang, X. Ding, H. Zhang, X. Li and H. Dong, *Food Hydrocoll.*, 2021, **115**, 106606.
88 S. Lin, X. Liu, Y. Cao, S. Liu, D. Deng, J. Zhang and G. Huang, *Food Chem.*, 2021, **339**, 128001.
89 S. Boufi, S. Bel Haaj, A. Magnin, F. Pignon, M. Impéror-Clerc and G. Mortha, *Ultrason. Sonochem.*, 2018, **41**, 327–336.
90 A. Agi, R. Junin, A. Gbadamosi, A. Abbas, N. B. Azli and J. Oseh, *Chem. Eng. Process.*, 2019, **142**, 107556.

91 E. C. Andrade, J. C. G. Louzada, S. C. Chelgani and L. d. S. Leal Filho, *J. Mater. Res. Technol.*, 2024, **33**, 6251–6262.
92 B. O. Otegbayo, A. R. Tanimola, J. Ricci and O. Gibert, *Gels*, 2024, **10**, 51.
93 W. Wang, Q. Wang and P. Wang, *Polym. J.*, 2025, **57**, 189–201.
94 Y. Chen, X. Han, D.-L. Chen, Y.-P. Ren, S.-Y. Yang, Y.-X. Huang, J. Yang and L. Zhang, *Foods*, 2024, **13**, 431.
95 J. Zhang, L. Tao, S. Yang, Y. Li, Q. Wu, S. Song and L. Yu, *Trends Food Sci. Technol.*, 2024, **144**, 104321.
96 D. Zhao, X. Zhang, Y. Zhang, E. Xu, S. Yan, H. Xu and M. Li, *Sustainable Food Technol.*, 2024, **2**, 615–634.
97 I. Sharma, A. Sinhmar, R. Thory, K. S. Sandhu, M. Kaur, V. Nain, A. K. Pathera and P. Chavan, *J. Food Sci. Technol.*, 2021, **58**, 2178–2185.
98 S. Wang, S. Wang, L. Liu, S. Wang and L. Copeland, *J. Agric. Food Chem.*, 2017, **65**, 1697–1706.
99 H. He, C. Chi, F. Xie, X. Li, Y. Liang and L. Chen, *Food Hydrocoll.*, 2020, **102**, 105637.
100 G. F. Nogueira, B. d. O. Leme, G. R. S. dos Santos, J. V. da Silva, P. B. Nascimento, C. T. Soares, F. M. Fakhouri and R. A. de Oliveira, *Polysaccharides*, 2021, **2**, 373–386.